Purdue University
Purdue e-Pubs

International Refrigeration and Air Conditioning Conference

School of Mechanical Engineering

2021

Experimental Investigation of Liquid and Vapor Mass Flows in a Parallel Tube Evaporator

Christian Kollik
Virtual Vehicle Research GmbH

Andreas Ennemoser
AVL List GmbH

Michael Lang
Schunk Carbon Technology GmbH

Raimund Almbauer
Schunk Carbon Technology GmbH

Kevin Wimmer
Schunk Carbon Technology GmbH

See next page for additional authors

Follow this and additional works at: https://docs.lib.purdue.edu/iracc

Kollik, Christian; Ennemoser, Andreas; Lang, Michael; Almbauer, Raimund; Wimmer, Kevin; Dür, Lukas; and Zainer, Christoph, "Experimental Investigation of Liquid and Vapor Mass Flows in a Parallel Tube Evaporator" (2021). *International Refrigeration and Air Conditioning Conference.* Paper 2263.
https://docs.lib.purdue.edu/iracc/2263

This document has been made available through Purdue e-Pubs, a service of the Purdue University Libraries. Please contact epubs@purdue.edu for additional information.
Complete proceedings may be acquired in print and on CD-ROM directly from the Ray W. Herrick Laboratories at https://engineering.purdue.edu/Herrick/Events/orderlit.html

Authors

Christian Kollik, Andreas Ennemoser, Michael Lang, Raimund Almbauer, Kevin Wimmer, Lukas Dür, and Christoph Zainer

This article is available at Purdue e-Pubs: https://docs.lib.purdue.edu/iracc/2263

Experimental Investigation of Liquid and Vapor Mass Flows in a Parallel Tube Evaporator

Christian KOLLIK[1]*, Andreas ENNEMOSER[2], Michael LANG[3], Raimund ALMBAUER[3], Kevin WIMMER[3], Lukas DÜR[3], Christoph ZAINER[3]

[1]Virtual Vehicle Research GmbH,
Inffeldgasse 21a, 8010 Graz, Austria
christian.kollik@v2c2.at

[2]AVL List GmbH,
Hans-List-Platz 1, 8010 Graz, Austria
andreas.ennemoser@avl.com

[3]Graz University of Technology, Institute of Internal Combustion Engines and Thermodynamics,
Inffeldgasse 19, 8010 Graz, Austria
michael.lang@ivt.tugraz.at
raimund.almbauer@ivt.tugraz.at
kevin.wimmer@ivt.tugraz.at
duer@ivt.tugraz.at
zainer@ivt.tugraz.at

* Corresponding Author

ABSTRACT

One of the major challenges in the evaluation of an evaporator heat exchanger in refrigeration cycles is to provide reasonable measurement data. Especially if the evaporator is multi-flow and therefore the measurement of the mass flow at one location and the evaluation of the overall energy balance is not sufficient for the characterization of the heat exchanger. In the present work, an evaporator of a capacity of approx. 1.2 kW, consisting of a distributor, a collector and four parallel evaporator tubes in which heat was introduced, was experimentally investigated. The four evaporator tubes made of stainless steel with an inner diameter of 2 mm, an outer diameter of 4 mm and a length of 800 mm were led out of the distributor and into the collector at a right angle at a distance of 90 mm from each other. All tubes form a plane. To keep the geometry of the joints as uniform as possible, commercially available fittings were used.

The evaporator was investigated as part of a refrigeration cycle with several adjustment possibilities like mass flow, subcooling, and pressure. To determine the mass flow and vapor quality distribution within the heat exchanger, each evaporator tube was divided into two heating sections of 400 mm and 200 mm length respectively with an intermediate measuring section of 200 mm for pressure and temperature. The first sections were heated by variable electrical heat loads, uniformly distributed over a length of 345 mm. The heat load was adjusted so that a slight superheating of approx. 4 K occurred at the outlet. In the second sections a constant electrical heat load was uniformly applied over a length of 150 mm. Assuming that a thermal equilibrium between the phases in the first sections is established, the heat loads can be used to draw conclusions about the respective mass flows of liquid refrigerant. In the second sections, the constant heat flow can be used to draw conclusions about the different total mass flows due to the different outlet temperatures. The measurements were carried out in our own laboratory for different vapor qualities from x=0 to x=0.3 and different overall total mass flows of the cycle ranging from 5, 7.5 and 10 kg/h to partly 20 kg/h. During the measurements, different inclinations of the evaporator relative to the horizontal plane were realized as well, so that a large number of measurement results were finally recorded. The measurement setup allows the evaluation of liquid and vapor refrigerant mass flow rates in each evaporator channel and makes a comparison between the sum of the four individual total mass flow rates and the overall total mass flow rate of the cycle possible. The results show the influence

of the variable gravity vector and flow velocity on the distribution. In the horizontal measuring point the tube furthest away from the distributor inlet exhibits the highest vapor quality of all 4 tubes, contrary to what was expected. Finally, the results are used to validate the simulation models of the industrial project partner.

1. INTRODUCTION

The battery cooling system is one of the most relevant components in electric or hybrid electric vehicles and has a significant energy consumption, weight and volume. In addition, at high ambient temperatures, there is often the need of battery cooling using a refrigeration cycle. Because of the limited space and weight for the refrigeration cycle evaporators with parallel cooling channels are the preferred choice. Uniform level of liquid refrigerant aggregation across the parallel cooling channels of the evaporator is very important for achieving consistent cooling of the battery, since in addition to the volume flow, the heat transfer is also significantly affected by the aggregate state (liquid, two-phase or gaseous). However, the refrigerant distribution into multiple cooling channels depends on the differing pressure losses of each channel due to the geometry, volume flows and vapor fraction. Moreover, accelerations (for example by cornering, speeding up or under braking) as well as road inclination can influence the refrigerant distribution.

Therefore, different test rig setups and measuring methods with the purpose of determining the two-phase distribution of a refrigerant in parallel evaporator tubes were developed in the past. In (Dong and Bean, 2006) a practical investigation of three coil inlet header configurations for microchannel evaporators was carried out. To evaluate refrigerant distribution uniformity air temperature differential across the coil was measured. For subcooled and superheated segments, heat transfer coefficient and heat transfer flow rate remain at relative lower level and therefore airflow temperature difference appears relatively small. Within the evaporating segment, the temperature difference of the air is significantly larger. Therefore, the airflow temperature differential indicates refrigerant status inside the microchannel tube. (Li and Hrnjak, 2015) presented a method to quantify the distribution of liquid refrigerant mass flow rate in a parallel flow microchannel heat exchanger from infrared images. A relationship was built between the liquid mass flow rate through each microchannel tube and the corresponding temperature difference on the air side. A thermocouple grid was used to measure the air temperature and an infrared camera was employed to provide the wall temperature measurement. As long as the boundary between single-phase region and two-phase region can be identified on the infrared image of the heat exchanger, the distribution of liquid refrigerant mass flow rate can be then determined. In (Endoh, 2016) an evaporator that has four passes of heater-heated tubes following four straight tubes was investigated. The powers of heaters for each pass of the evaporator were controlled in such a way that the temperatures of superheated vapor at the outlet of each pass were set at a predetermined value. Differential pressures of superheated vapors in straight tubes at the outlet of each pass were measured for calculating refrigerant mass flow rates for each tube with a Blasius equation for friction factor. With the electric power of the heaters for the heater-heated tubes and the mass flow rate of each tube the enthalpy and therefore the vapor quality x at the inlet of the tubes was calculated. Therefore, the mass flow rate of liquid and vapor phase for each tube was determined. In (Byun and Kim, 2011) refrigerant R-410a flow distribution was experimentally studied in a test section simulating a parallel flow heat exchanger having vertical headers with two pass configuration. In their work flow rate of every other channel of the evaporator is measured. In the following condenser cooling water cools the refrigerant to a subcooled temperature. For the cooling water, temperature at inlet and outlet and the mass flow is measured. For the refrigerant the mass flow of the channel is known from the measurement in the evaporator. With this information the vapor quality at the evaporator outlet is calculated. The evaporator is heated by a heater and as the applied power to the heater is measured the quality at the inlet of the evaporator channel can be calculated. An experimental investigation of pressure drop and void fraction in aluminium microchannel tubes was conducted in (Payne et al., 2000) for a variety of flow conditions. Refrigerant quality in the microchannels was measured by trapping the refrigerant in the channels by closing both ends of the channel with pneumatic cylinders equipped with blades. (Bowers et al., 2012) outline general trends in refrigerant flow distribution in microchannel evaporators taking into account various heat exchanger orientations. The refrigerant flow distribution in all cases was analysed using infrared thermography and quantified with a statistical methodology for infrared thermography outlined in (Bowers et al., 2010).

The intention of this work is to find a time- and cost-efficient method to successfully measure the two-phase refrigerant distribution in the parallel evaporation channels during various inclinations of the distributor and evaporation channels to generate evaluation data for the simulation model.

2. EXPERIMENTAL SETUP

2.1. Test Rig Architecture and Methodology

The implemented test rig architecture in Figure 1 consists of five components: condenser, reservoir, sub cooler, magnetic gear pump and a pre-heater. This configuration deviates considerably from a standard compression refrigeration cycle and is aimed to provide a constant saturation pressure between 3 and 3.5 bar and vapor qualities between 0 and 0.5 at the inlet of the test section. Following the components of the test rig are described in detail.

The main purpose of the reservoir in Figure 2 is to provide stable thermodynamic conditions within the refrigeration cycle and to act as a refrigerant buffer. The reservoir consists of two concentric steel cylinders. The inner cylinder contains the refrigerant (approximately 5 kg of R134a at a filling level of around 50%). The void space between the inner cylinder and the outer shell is filled with brine conditioned to a certain temperature, thereby adjusting the refrigerant's saturation temperature and pressure to desired levels. The test rig is designed to provide saturation temperatures between -5 °C and 25 °C which corresponds to saturation pressures between 2.4 bar and 7 bar.

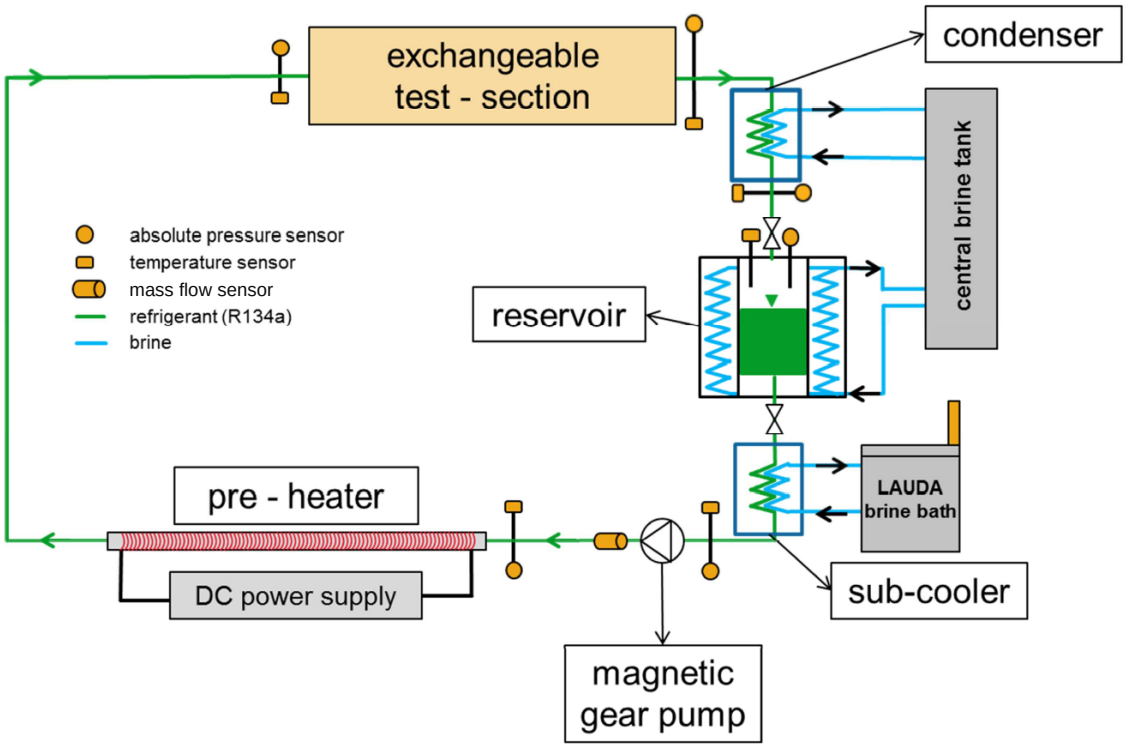

Figure 1: Test rig architecture

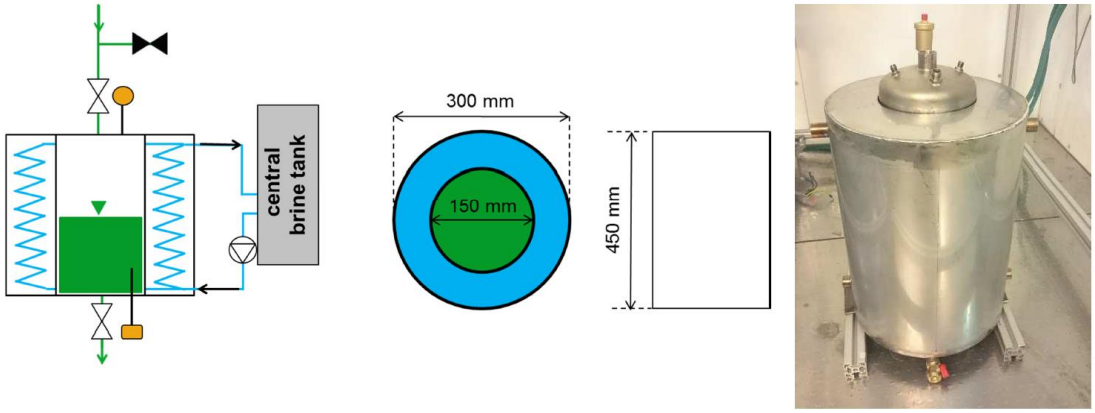

Figure 2: Test rig reservoir

Just after the reservoir a brazed plate heat exchanger (brine – refrigerant heat exchanger, Figure 3) is installed in order to bring the saturated refrigerant into a subcooled state. Subcooling the refrigerant is necessary for a couple of reasons. First and foremost a subcooled refrigerant state is important in order to exactly determine the refrigerants enthalpy at the entrance of the pre-heating section (by means of pressure and temperature measurements) and to dial in a certain vapor quality at the test section entrance by adjusting the heat load at the pre-heater. Furthermore, a completely vapor free flow rate through the Coriolis sensor is important for usable and stable mass flow measurements, and finally a bubble free volume flow through the magnetic gear pump is equally important for a stable mass flow rate and the magnetic gear pump's longevity. The refrigerant capacity for subcooling is supplied by a brine temperature bath with a cooling capacity of 180 W at -10 °C, which is sufficient to provide subcooling of 10 K to a refrigerant mass flow rate of 30 kg/h at 9 °C saturation temperature. The magnetic gear pump in Figure 3 is able to provide refrigerant mass flow rates between 1 and 30 kg/h and thus can cover all necessary operation points for the given test specimens.

The pre-heater in Figure 4 consists of a 1.5 m long section with heating wire wound around the refrigerant tube. Through temperature and pressure measurements at the pre-heater inlet the refrigerant's enthalpy can be calculated (refrigerant entering the pre-heater is in a subcooled state) and consequently a desired vapor quality at the test section inlet can be provided by adjusting the heating load at the heating wire by means of a DC power supply. The pre-heater is divided into three heating sections that are operated in electrical parallel operation. Across each of the three heating sections, current and voltage measurements are taken in order to determine the exact heat load provided by the DC power supply. Several temperature sensors are applied directly on the coils, on the inside of the insulation layer and on the outside to monitor coil temperatures and to calculate heat losses/gains from the ambient.

The condenser (brazed plate heat exchanger, Figure 5) sits between the test section and the reservoir and acts as a heat sink in order to fully condense the refrigerant vapor exiting the test section. The condenser is fed with brine at the same temperature as the reservoir is. Temperature and pressure measurements are taken at the condenser outlet in order to determine if the refrigerant is in liquid state.

Figure 3: Brazed plate HX (brine refrigerant) for subcooling and magnetic coupled gear pump

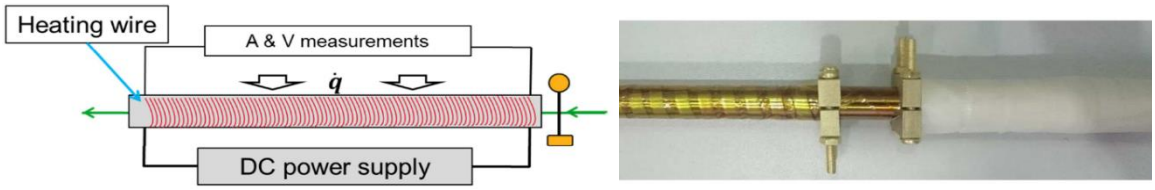

Figure 4: Schematics of pre-heater (left); heating wire and electrical insulation tape with electrical connection clamps and first thermal insulation layer (right)

Figure 5: Schematics of condenser integration and image of condenser

2.2. Test Evaporator

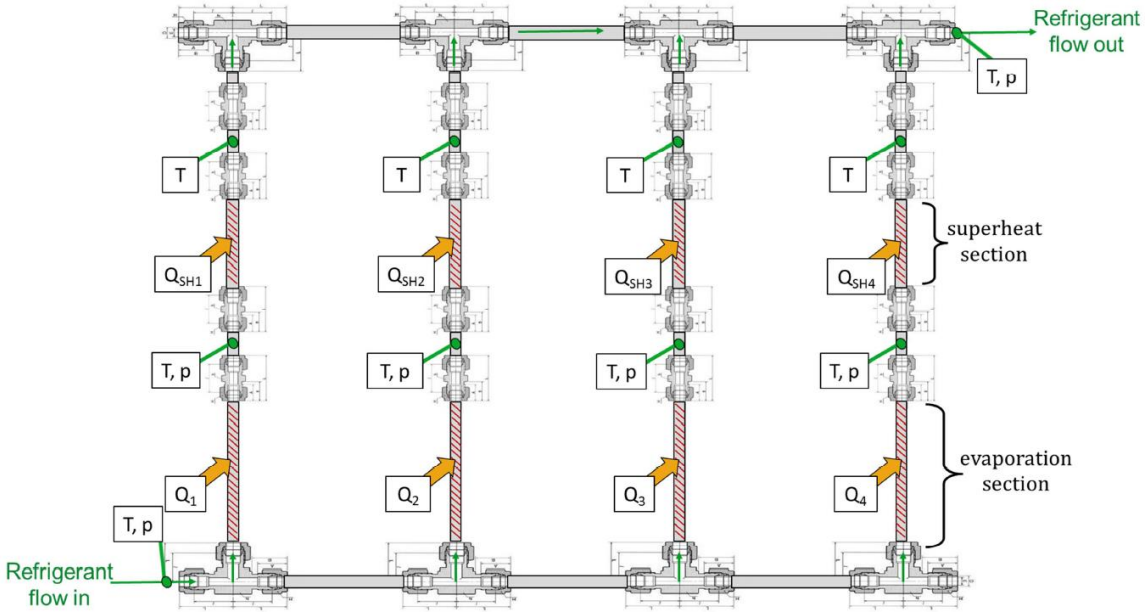

Figure 6: Schematics of the test evaporator for vapor quality distribution measurements

The schematic drawing of the test evaporator is shown in Figure 6. The evaporator is built with connectors for simplicity reason and to avoid welding joints that can adversely influence the refrigerant flow (e.g. due to bending of tubes occurring during welding). Each evaporator tube consists of an evaporation section, followed by a measurement section where refrigerant pressure and temperature are measured, and a superheat section, followed by a measuring section where only refrigerant temperature is measured. Both, evaporation and superheat sections are heated by means of a heating wire wound around the tube, just like in the case of the pre-heater of the test rig in Figure 4. Heat input for each evaporation section is separately controlled by DC power supplies, while all four superheat sections are controlled by only one power supply. Additionally, to the afore mentioned measuring points, pressure and temperature at the evaporator inlet and outlet are also measured.

2.3. Measurement Principle

Since it is not possible to measure liquid and gas mass flow rates at each of the parallel evaporator tubes (e.g. with a Coriolis mass flow sensor) a different way had to be found. For this test evaporator, measuring the gas and liquid mass flow distribution was done indirectly. With measurement of the heat flux input in each evaporation and superheat section as well as refrigerant temperature and pressure measurements the liquid and gas mass flow rate at each evaporator tube inlet can be calculated. The calculation is carried out with the governing equations below. During test rig measurements the heat fluxes at all four evaporation sections are independently controlled from each other in order to reach superheat levels of the refrigerant at the evaporation section outlet of around 4 K. At the superheat sections the same amount of heat flux is applied to further superheat the refrigerant at levels around 35 K. With the equations (1), (2) and (3) the total mass flow rate in each of the 4 tubes can be calculated, since the state of the refrigerant at the superheat section inlet and outlet is determined by temperature and pressure measurements (refrigerant is in a single-phase superheated state).

$$\dot{Q}_{Net,SH,i} = \dot{m}_{t,i} \cdot (h_{SH\,out,i} - h_{SH\,in,i}) \tag{1}$$

$$\dot{Q}_{Net,SH,i} = q_{elec,SH,i} \cdot L_{SH} - \dot{Q}_{losses,SH,i} \tag{2}$$

$$\dot{m}_{t,i} = \frac{\dot{Q}_{Net,SH,i}}{h_{SH\,out,i} - h_{SH\,in,i}} \tag{3}$$

With equation (4), (5) and (6) the liquid mass flow rate is calculated, with the assumption, that the heat flux applied at the evaporation sections is fully absorbed by the liquid portion of the mass flow rate of each of the parallel tubes.

The calculated liquid mass flow is corrected slightly by the portion of the heat flux, which is responsible for superheating the refrigerant in the evaporation section (second term of the numerator in equation (6)).

$$\dot{Q}_{Net,evap,i} = \dot{m}_{l,i} \cdot \left(h_{in,v} - h_{in,l}\right) + \dot{m}_{t,i} \cdot \left(h_{evap,out,i} - h_{in,v}\right) \tag{4}$$

$$\dot{Q}_{Net,evap,i} = q_{elec,evap,i} \cdot L_{evap} - \dot{Q}_{losses,evap,i} \tag{5}$$

$$\dot{m}_{l,i} = \frac{\dot{Q}_{Net,evap,i} - \dot{m}_{t,i} \cdot \left(h_{evap,out,i} - h_{in,v}\right)}{h_{in,v} - h_{in,l}} \tag{6}$$

With the knowledge of liquid and gas mass flow rate at each evaporator tube, the different vapor qualities at the tube inlets can be calculated with equation (7).

$$x_i = \frac{\dot{m}_g}{\dot{m}_g + \dot{m}_l} \tag{7}$$

Different inclinations of the distributor/collector and evaporation tubes were tested in order to simulate longitudinal and lateral accelerations of the vehicle. Figure 7 shows the schematic of the test evaporator with a cartesian coordinate system from the bird's eye view. Initial position for both, evaporator tubes and distributor/collector, is a horizontal orientation meaning 0° rotation about x and y axis. Inclinations of the distributor/collector would mean a rotation about the x-axis. A negative rotation (e.g. -15°) around the x-axis would result in the inlet of the distributor being higher than the outlet of the collector (with no rotation about the y axis). Therefor the distributor/collector would be sloped downward from evap_1 to evap_4. A positive rotation about the x axis on the other hand, would result in an upward sloped distributor/collector (inlet of the distributor lower than outlet of collector). Inclinations of the parallel evaporation tubes are achieved by rotations about the y axis. A positive rotation would lead to a downward slope of the evaporation tubes (seen in refrigerant flow direction) and a negative rotation in an upward slope (with 0° rotation about the x axis). In this work, rotations about the x and y axis have only been investigated separately from each other and not together (e.g. 0° about the x axis and +15° about the y axis).

With the built-up evaporator shown in Figure 8, test rig measurements have been carried out in order to calculate the vapor fraction (x_i) distribution in the 4 parallel evaporation tubes. Different inclinations of the evaporator tubes and distributor/collector were realized by panning the frame on which the test section is mounted on.

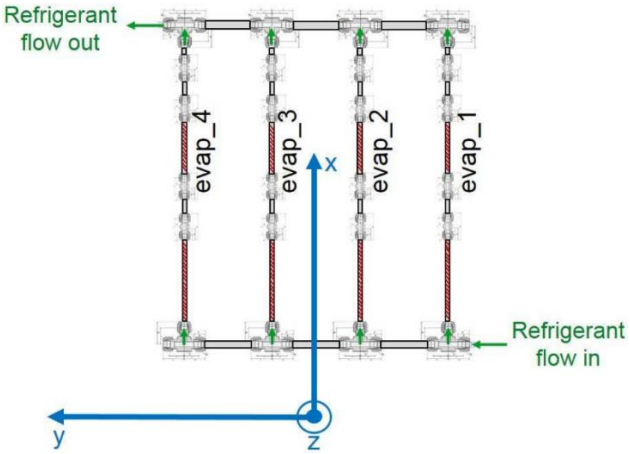

Figure 7: Orientation of the test evaporator

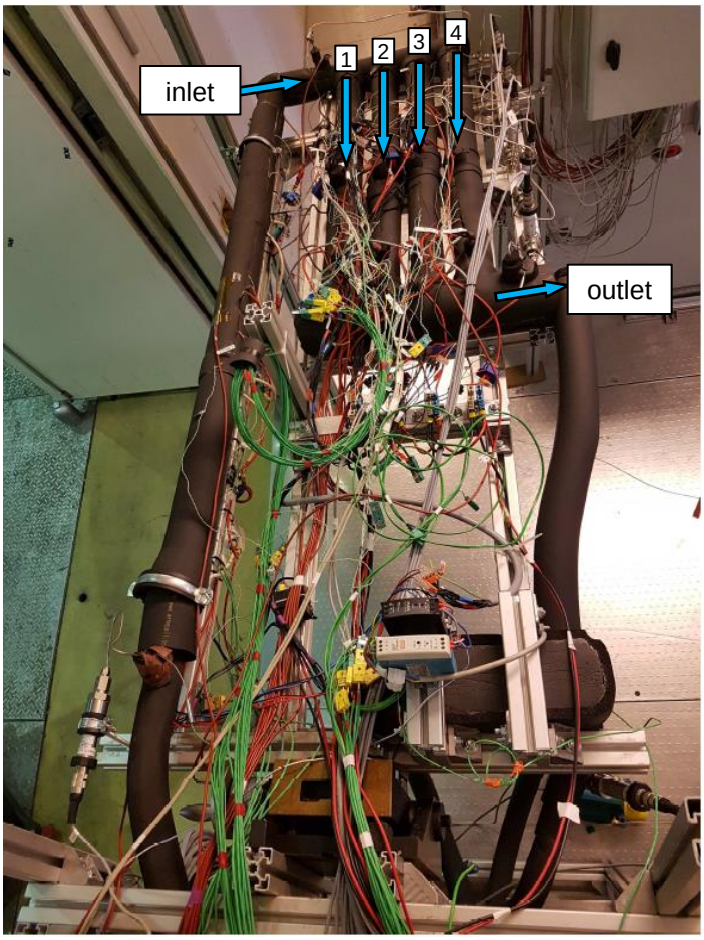

Figure 8: Test evaporator on the rotatable frame with pre-heater and condenser

3. RESULTS

As described tests with different rotations about the x and y-axis were carried out. Moreover, the effect of different mass flow rates (5, 7.5, 10, 15 and 20 kg/h) as well as different vapor qualities (x=0, x=0.15, x=0.30) were investigated. The refrigerant pressure for all measurements was 3.5 bar. In total 62 different measuring points were carried out. Table 1 gives an overview about the set parameters of these measurements.

Table 1: Overview of all measuring points carried out

		Mass flow 5 [kg/h]			Mass flow 7.5 [kg/h]			Mass flow 10 [kg/h]			Mass flow 15 [kg/h]			Mass flow 20 [kg/h]		
Rotation [°]		Vapor quality [-]			Vapor quality [-]			Vapor quality [-]			Vapor quality [-]			Vapor quality [-]		
x-axis	y-axis	0	0.15	0.30	0	0.15	0.30	0	0.15	0.30	0	0.15	0.30	0	0.15	0.30
0	0	✓	✓	✓	✓	✓	✓	✓	✓	✓		✓	✓		✓	✓
15	0	✓	✓	✓	✓	✓	✓	✓	✓	✓						
30	0	✓	✓	✓	✓	✓	✓	✓	✓	✓						
-15	0	✓	✓		✓	✓	✓	✓	✓	✓						
0	10				✓	✓	✓	✓	✓	✓						
0	-10	✓	✓	✓	✓	✓	✓	✓	✓	✓						
0	-90	✓	✓	✓	✓	✓	✓	✓		✓						

Deviations for the vapor qualities 0.15 and 0.3 appeared in the measurements. Therefore, the actual vapor qualities are shown in the results. Furthermore, it should be stated, that in a few cases, due to measuring uncertainties, calculations of the vapor quality lead to a negative vapor quality in the evaporator tubes. This is physical not possible, but for better comparison negative x values are not set to zero.

The results (vapor qualities, liquid-, gas- and total mass flow rates) for the horizontal measurements (0° rotation about x- and y-axis) for mass flows of 5, 7.5 and 10 kg/h and vapor qualities of 0, 0.15 and 0.30 are illustrated in Figure 9, 10, 11 and 12. The bars in the figures are arranged in the same order as shown in Figure 7, so the first bar from the left for each measuring point represents a certain value at evaporation tube 4. CFD simulations were carried out as well but their discussion is not topic of this work. However, some measurement results are compared with the simulation results just in terms of plausibility.

For all measuring points, except at a vapor fraction of 0 at the distributor inlet, evaporator tube 4 exhibits the highest vapor quality of all 4 tubes, contrary to the CFD simulations. While liquid mass flow is lowest for tube 4 at vapor qualities of 0.15 and 0.30, reducing the vapor fraction of the refrigerant at the distributor inlet to 0 (only liquid refrigerant) leads to a much more uniform liquid mass flow distribution as shown in Figure 10. Despite uneven liquid mass flow distribution for measuring points with x>0 at the distributor inlet, the total mass flow distribution at each evaporation tube appears to be more uniform than expected. The horizontal measurements have revealed an opposing trend to the CFD simulation results where kinetic effects lead to the highest liquid mass flow rates at tube 4 in comparison to tube 1-3. At the horizontal test rig measurements, vapor qualities at tube 4 were mostly much higher than for tube 1-3, except for vapor fractions of 0 at the distributor inlet. Since refrigerant flow velocities in the distributor tube are quite low (especially at low vapor qualities) kinetic effects most probably play a minor role. Therefore, a slight miss-alignment of the distributor orientation of ± 0.5 degrees could already lead to diverging results from what would be expected of a fully horizontal configuration.

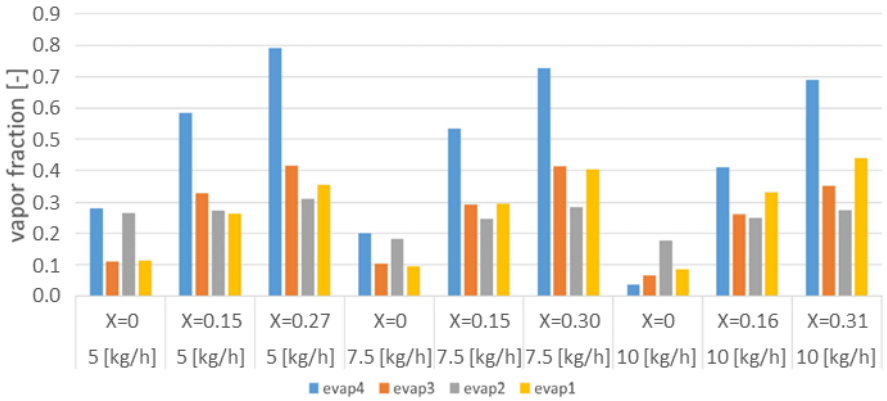

Figure 9: Vapor quality distribution for horizontal measurement at 3.5bar

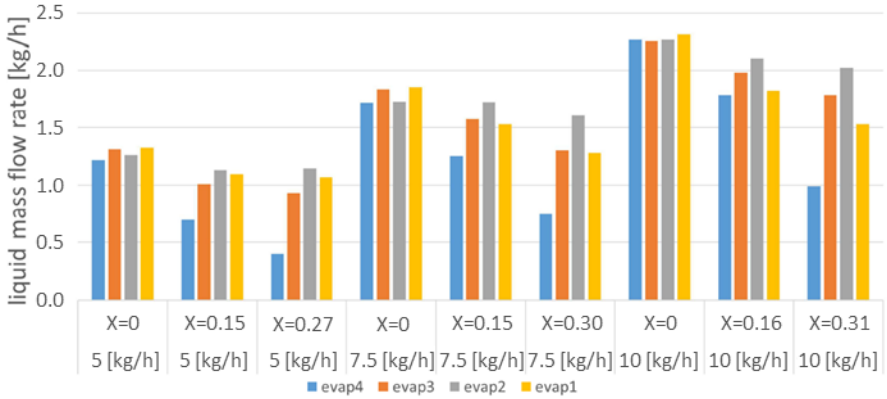

Figure 10: Liquid mass flow distribution for horizontal measurement at 3.5bar

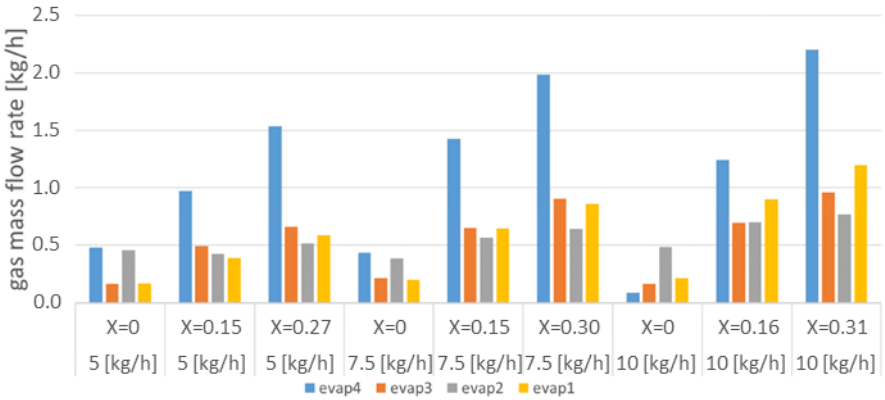

Figure 11: Gas mass flow distribution for horizontal measurement at 3.5bar

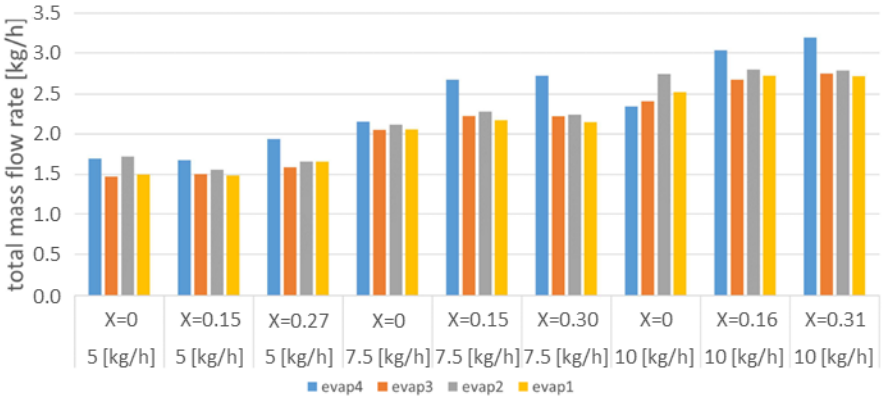

Figure 12: Total mass flow distribution for horizontal measurement at 3.5bar

The further measuring points with rotation about the x-axis or y-axis show continuously expectable results. Positive rotations of 15° and 30° about the x-axis result in high vapor qualities in tube 4 as the gas phase is expected to rise to the top (tube 4). A negative rotation of 15° about the x-axis results in a distributor sloped downward from tube 1 to tube 4 and therefore in higher vapor qualities for tube 1.

For a rotation of 10° about the y-axis the evaporator tubes are downward sloped. Vapor quality at tube 4 turns out to be the highest. For a negative rotation of 10° about the y-axis tube 1 experiences the highest vapor quality for measuring points with vapor qualities at the distributor inlet greater than 0. This trend intensifies for the vertical case (-90° rotation about the y-axis). Vapor qualities at tube 1 are by far the highest of all measuring points with vapor qualities at the distributor inlet greater than 0.

For all measuring points adjusting the vapor quality at the distributor inlet to 0 (only liquid refrigerant) harmonizes the vapor quality distribution at all four evaporation tubes.

4. CONCLUSIONS

A new methodology for measuring the vapor quality distribution in a parallel tube evaporator is developed and measuring points at different rotations of the evaporator, different mass flow and vapor qualities are carried out. This new methodology measures the liquid and gas mass flows of the evaporator tubes indirectly by slightly superheating the two-phase refrigerant in a first section and by further heating the superheated refrigerant in a second section. With a calculation of the governing equations the liquid and the gas mass flows and therefore the total mass flows and the vapor qualities of the tubes are determined.

The method has delivered interesting and useful results for the two-phase refrigerant distribution in parallel evaporator tubes at different inclinations. However, it has been shown, that measurements with a horizontal orientation of the

distributor are more or less sensitive (additionally depending on the orientation of the evaporator tubes) to slight misalignments (±0.5°) since gravitational effects upon the liquid phase could lead to implausible test rig results as in the horizontal case (0° about x- and y-axis). Therefore, test rig data for the purpose of CFD model validation should be used with some degree of scrutiny.

NOMENCLATURE

DC	Direct current		**Subscript**	
HX	Heat exchanger		Net	net
CFD	Computational fluid dynamics		SH	superheated
$\dot{Q}$	Heat flow	(W)	i	section
$\dot{m}$	Mass flow	(kg/s)	t	total
h	Enthalpy	(J/(kg))	out	outlet
q	Specific heat load	(W/m)	in	inlet
L	Length	(m)	elec	electric
x	Vapor quality	(-)	losses	losses
			evap	evaporator
			l	liquid
			v	vapor
			g	gas

REFERENCES

Bowers, C. D., Mai, H., Elbel, S., & Hrnjak, P. S. (2012). Refrigerant Distribution Effects on the Performance of Microchannel Evaporators. *International Refrigeration and Air Conditioning Conference, Purdue*.

Bowers, C. D., Wujek, S. S., & Hrnjak, P. S. (2010). Quantification of Refrigerant Distribution and Effectiveness in Microchannel Heat Exchangers Using Infrared Thermography. *International Refrigeration and Air Conditioning Conference, Purdue*.

Byun, H. W., & Kim, N. H. (2011). Refrigerant distribution in a parallel flow heat exchanger having vertical headers and heated horizontal tubes. *Experimental Thermal and Fluid Science*, *35*(6), 920–932. https://doi.org/10.1016/j.expthermflusci.2011.01.011

Dong, Z. G., & Bean, J. (2006). Experimental Research and CFD Simulation on Microchannel Evaporator Header to Improve Heat Exchanger Efficiency. *International Refrigeration and Air Conditioning Conference, Purdue*.

Endoh, K. (2016). Refrigerant Distribution Characteristics in Vertical Header of Flat-Tube Heat Exchanger. *International Refrigeration and Air Conditioning Conference, Purdue*.

Li, H., & Hrnjak, P. (2015). Quantification of liquid refrigerant distribution in parallel flow microchannel heat exchanger using infrared thermography. *Applied Thermal Engineering*, *78*, 410–418. https://doi.org/10.1016/j.applthermaleng.2015.01.003

Payne, W. T., Nino, V. G., Hrnjak, P. S., & Newell, T. A. (2000). Void fraction and pressure drop in microchannels. *Air Conditioning and Refrigeration Center. College of Engineering. University of Illinois at Urbana-Champaign.*

ACKNOWLEDGEMENT

This work originated in a project for the development of battery cooling systems in a consortium of the AVL-List GmbH (AVL), Virtual-Vehicle (ViF) and Graz University of Technology (TUG).

The publication was supported by the Virtual Vehicle Research GmbH in Graz, Austria. The authors would like to acknowledge the financial support within the COMET K2 Competence Centers for Excellent Technologies from the Austrian Federal Ministry for Climate Action (BMK), the Austrian Federal Ministry for Digital and Economic Affairs (BMDW), the Province of Styria (Dept. 12) and the Styrian Business Promotion Agency (SFG). The Austrian Research Promotion Agency (FFG) has been authorised for the programme management. They would furthermore like to express their thanks to their supporting industrial and scientific project partners, namely the AVL-List GmbH and to the Graz University of Technology.